final report

Project code: P.PSH.1135

Prepared by: Ian Woodhead
Lincoln Agritech Limited

Date published: 13 May 2019

PUBLISHED BY
Meat and Livestock Australia Limited
Locked Bag 1961
NORTH SYDNEY NSW 2059

Bessel Beam Microwave Platform for Livestock and Carcase Surface Fat Depth Imaging – MLA Public

This is an MLA Donor Company funded project.

Meat & Livestock Australia acknowledges the matching funds provided by the Australian Government to support the research and development detailed in this publication.

Executive summary

The project planned to run from October 2018 until November 2019 but the project was terminated by Meat & Livestock Australia due to research priorities.

This document provides a summary of work undertaken for MLA during by Lincoln Agritech between the dates 1 October 2018 – 26 November 2018. Note that there was a two-week shutdown from 29 October 2018, after which work resumed until the termination date.

This project was undertaking the underpinning research and development of a prototype for the first application of an "on-the-hoof" body condition sensor. It planned to be a valuable stock management tool for production, livestock health, and nutrition, which would be developed in collaboration with our industry partners. Bessel beams which are a relatively new discovery, is a narrow, non-divergent beam of microwave radio waves, and are well-suited to sensing because of the consistent narrow beam. Further, the signals scattered from objects or layers provide information about their size and the material from which they are made. The research planned to extend knowledge of how Bessel beams behave, as well as how they can be used to provide high resolution data.

For live animal surface fat depth assessment, and fat coverage in carcases, the project was to develop a sensor which would collect several tens of fat depth measurements from the flank of the passing animal, and exploit the following properties of Bessel beams: low power (safe), narrow (~30mm) central non-diffracting (somewhat parallel) beam, range of ~1 metre, scattering properties that are amenable to distinguishing fat layers.

The largest scattered signal will be from the skin surface and the next from the fat-to-muscle layer. The phase lags between transmission and these two dominant reflections will represent transmitter to skin and transmitter to muscle distances respectively. Spurious signals, such as from the outer wool profile of wet sheep or from multiple skin-muscle reflections, are expected to be easily distinguished; wool reflections will occur before the stronger skin reflection and secondary or multi¬path reflections will be strongly attenuated.

Lincoln Agritech had already completed the developed and proof of concept via simulation, design, and preliminary testing, the theoretical and practical basis for generating a range of Bessel beam geometries using a sparse circular patch array antenna.

Table of contents

1 Background

The project planned to run from October 2018 until November 2019 but the project was terminated by Meat & Livestock Australia due to research priorities.

This document provides a summary of work undertaken for MLA during by Lincoln Agritech between the dates 1 October 2018 – 26 November 2018. Note that there was a two-week shutdown from 29 October 2018, after which work resumed until the termination date.

This project is undertaking the underpinning research and development of a prototype for the first application of an "on-the-hoof" body condition sensor. This will be a valuable stock management tool for production, livestock health, and nutrition, which will be developed in collaboration with our industry partners. Bessel beams which are a relatively new discovery, is a narrow, non-divergent beam of microwave radio waves, and are well-suited to sensing because of the consistent narrow beam. Further, the signals scattered from objects or layers provide information about their size and the material from which they are made. The research will extend knowledge of how Bessel beams behave, as well as how they can be used to provide high resolution data.

For live animal surface fat depth assessment, and fat coverage in carcases, the project will develop a sensor which will collect several tens of fat depth measurements from the flank of the passing animal, and exploit the following properties of Bessel beams: low power (safe), narrow (~30mm) central non-diffracting (somewhat parallel) beam, range of ~1 metre, scattering properties that are amenable to distinguishing fat layers.

The largest scattered signal will be from the skin surface and the next from the fat-to-muscle layer. The phase lags between transmission and these two dominant reflections will represent transmitter to skin and transmitter to muscle distances respectively. Spurious signals, such as from the outer wool profile of wet sheep or from multiple skin-muscle reflections, are expected to be easily distinguished; wool reflections will occur before the stronger skin reflection and secondary or multi¬path reflections will be strongly attenuated.

Lincoln Agritech have already completed the develop and proof of concept via simulation, design, and preliminary testing, the theoretical and practical basis for generating a range of Bessel beam geometries using a sparse circular patch array antenna.

2 Project objectives

- Complete the Bessel beam microwave transmit/receive antenna validation
- Complete the basic Bessel beam scattering model for layered dielectrics
- Test the model response to a range of dielectric layers (including curvature, roughness, angles)
- Complete measurement system and test/refine in the lab
- Configure existing componets to enable field testing on live animals.

3 Methodology

3.1 Milestone 1 – Australian Market

3.1.1 Preliminary planning

Lincoln Agritech discussed arrangements internally, identified staff and provisionally determined the first set of visits early January 2019 and had identified Dr Jess Roberts, Lecturer in Precision Agriculture at Marcus Oldham College, Geelong and Jonathan England of AgInnovate and a recognised leader in sheep production systems.

The rest of the methodology has not been completed due to the contract being terminated. See the results section for additional methodology for individual milestones.

4 Results

4.1 Milestone 2 – Core Microwave Platform

4.1.1 Antenna Design

Design of a single antenna element for the frequency bandwidth between 1 – 10 GHz to optimize the directivity and pattern stability.

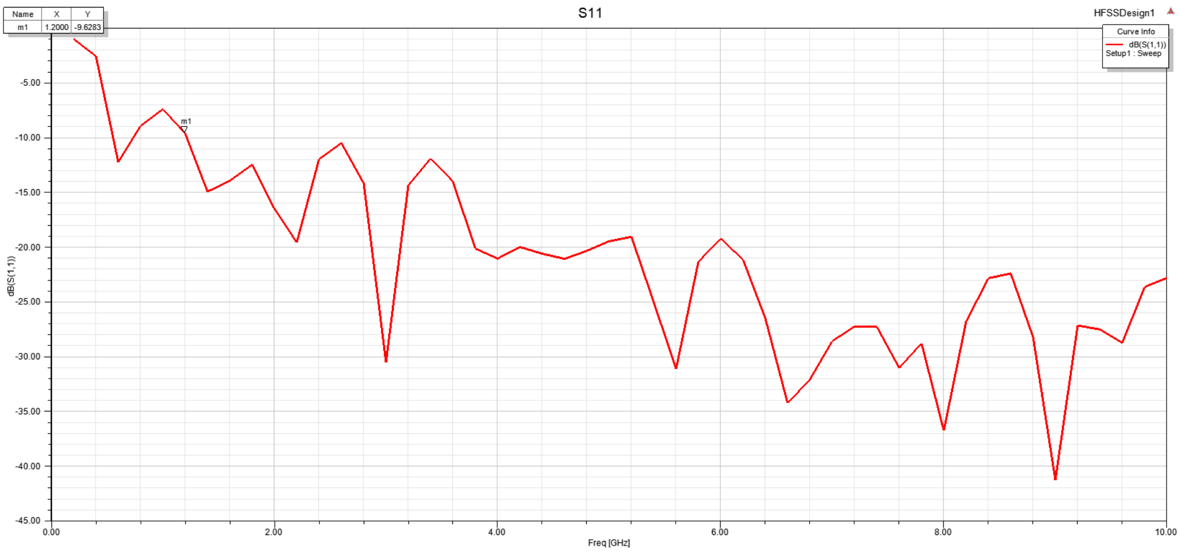

Fig. 1: Simulated S11 of the antenna indicating that antenna operation starts at 1.2 GHz.

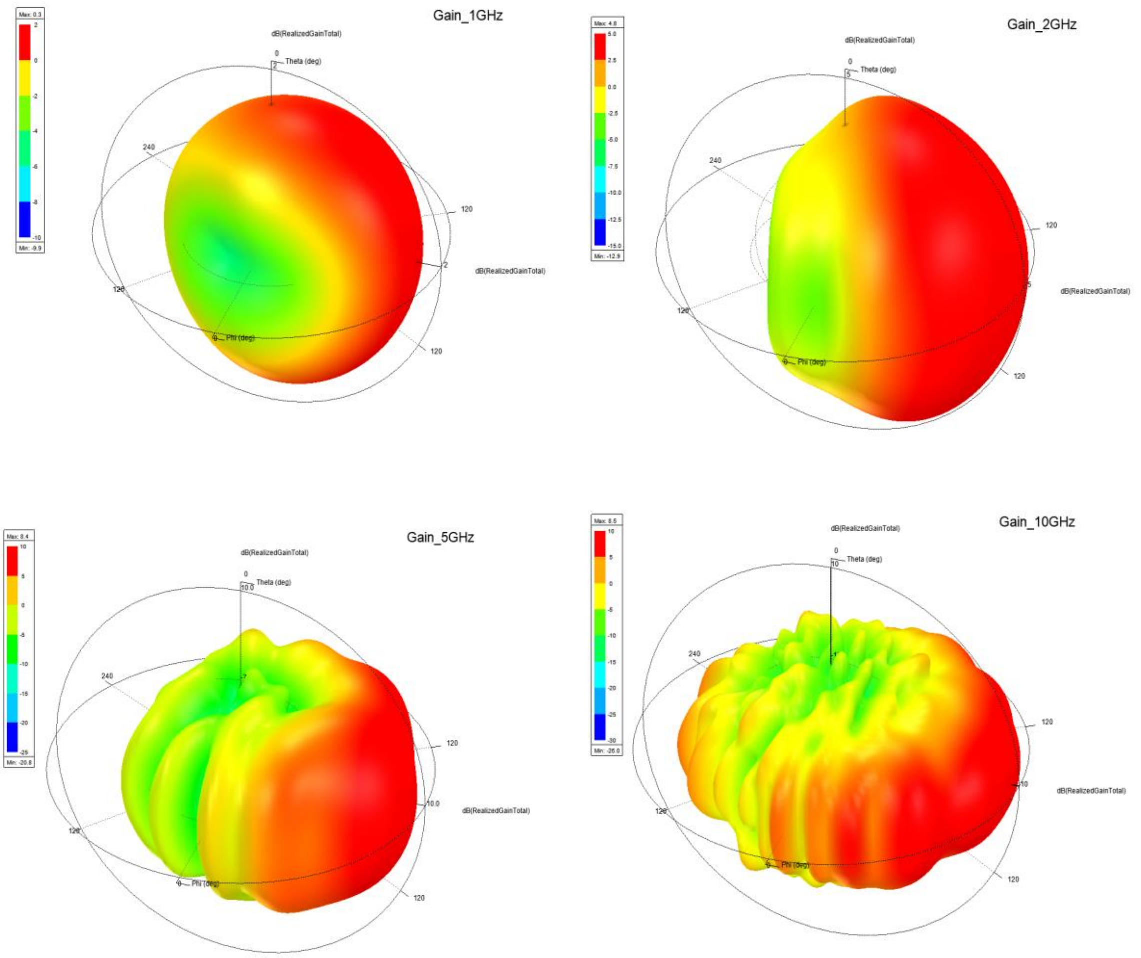

Fig. 2: Simulated radiation patterns show that antenna achieves a good main lobe in radiation patterns for all frequencies within the operating range.

4.1.2 Single Power Splitter Design

The power divider design involved analytical computation of the required impedance and resistance values required for a wideband Wilkinson divider. These values were then optimised with schematic simulations using behavioural models of ideal resistors and transmission lines. The optimised values were then ported to an electromagnetic wave simulation software, and the actual layout of the power divider drawn and simulated with both ideal and non-ideal circuit conditions. The diagrams below show the simulations and result in different stages of the design:

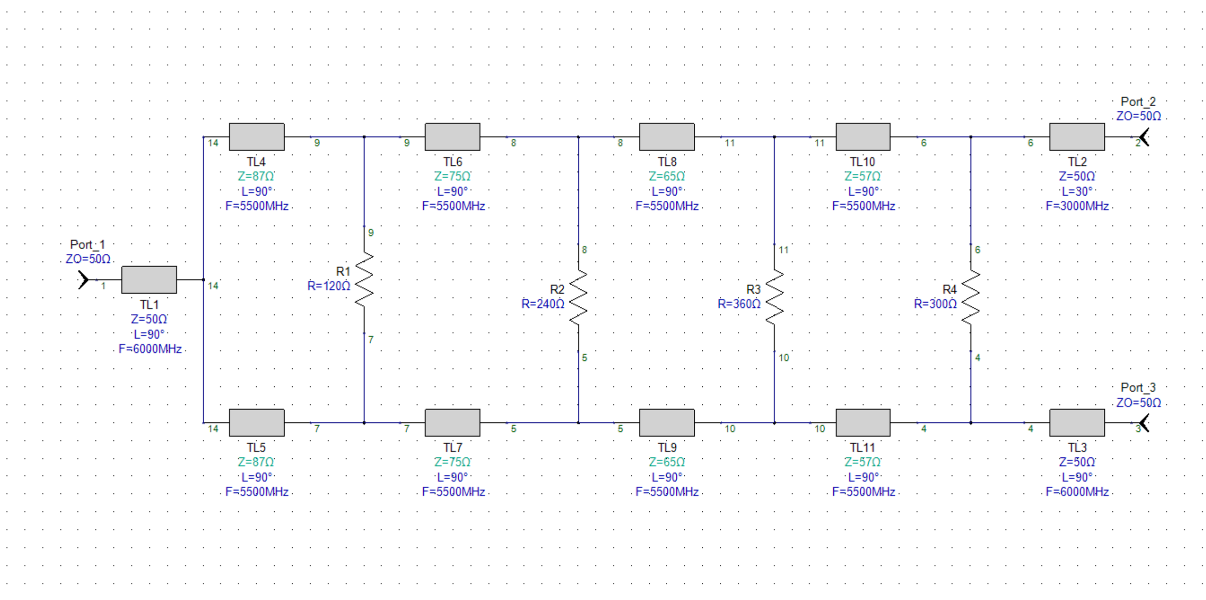

Fig. 3: Schematic level simulation of the power divider.

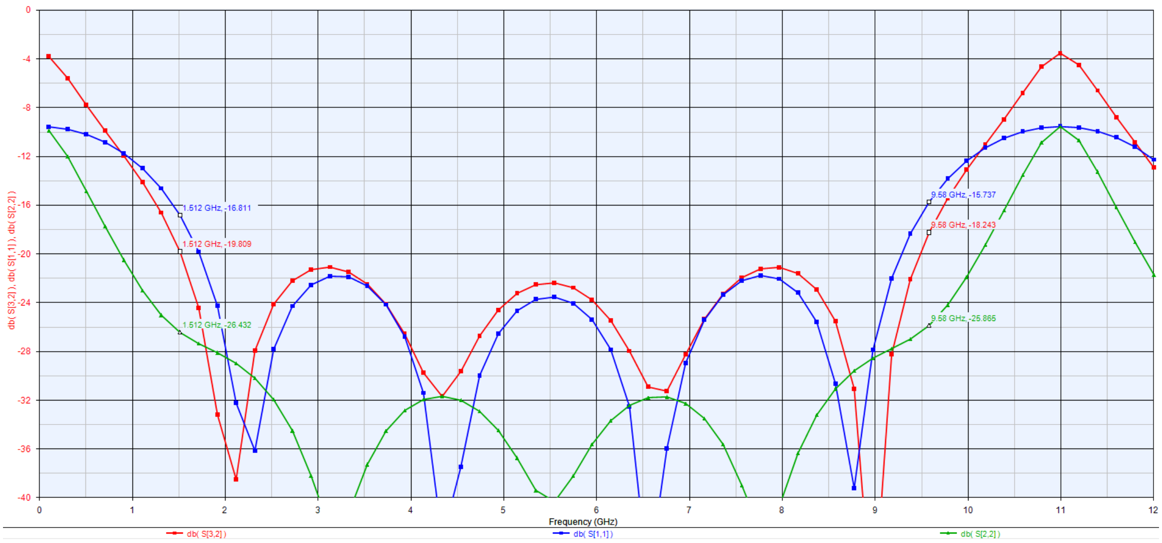

Fig. 4: Return loss and isolation for the schematic level simulation of the power divider.

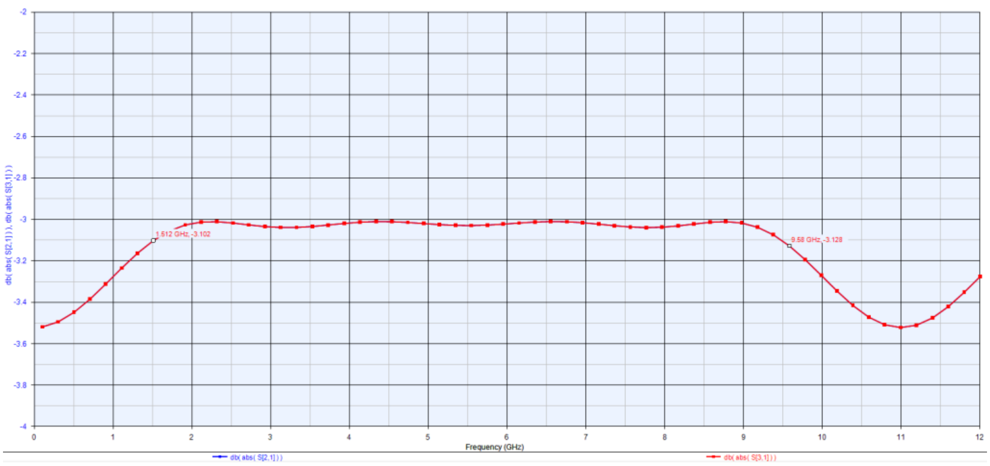

Fig. 5: Insertion loss for the schematic level simulation of the power divider.

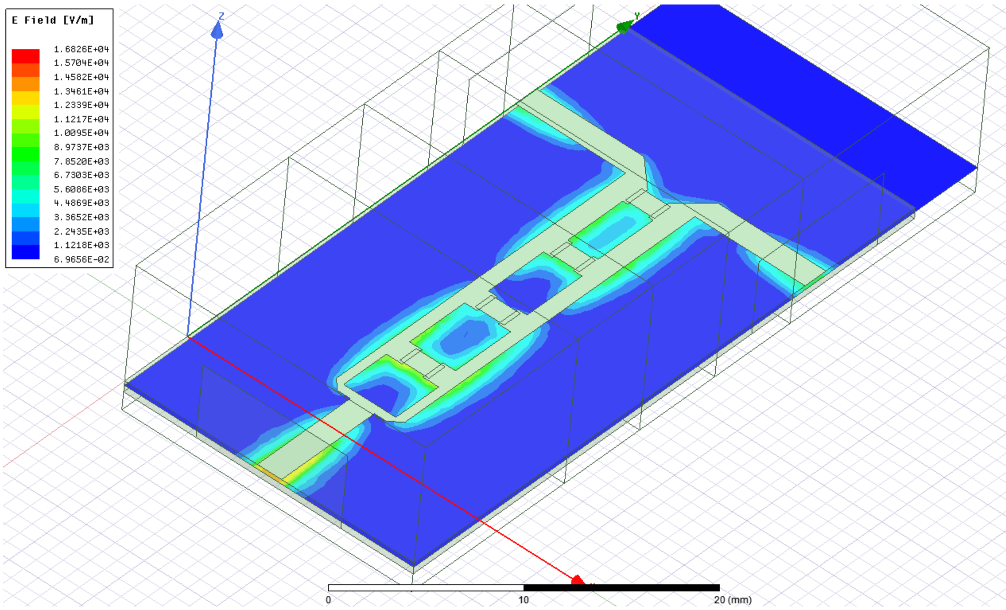

Fig. 6: Typical electrical field strength for the power divider.

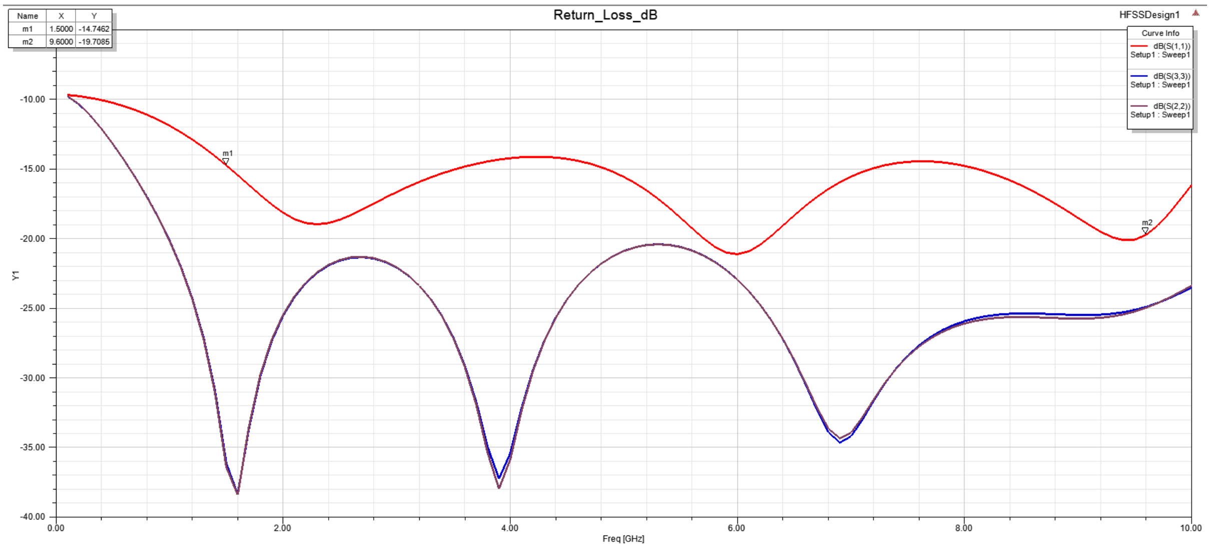

Fig. 7: Simulated results for return losses in the power divider.

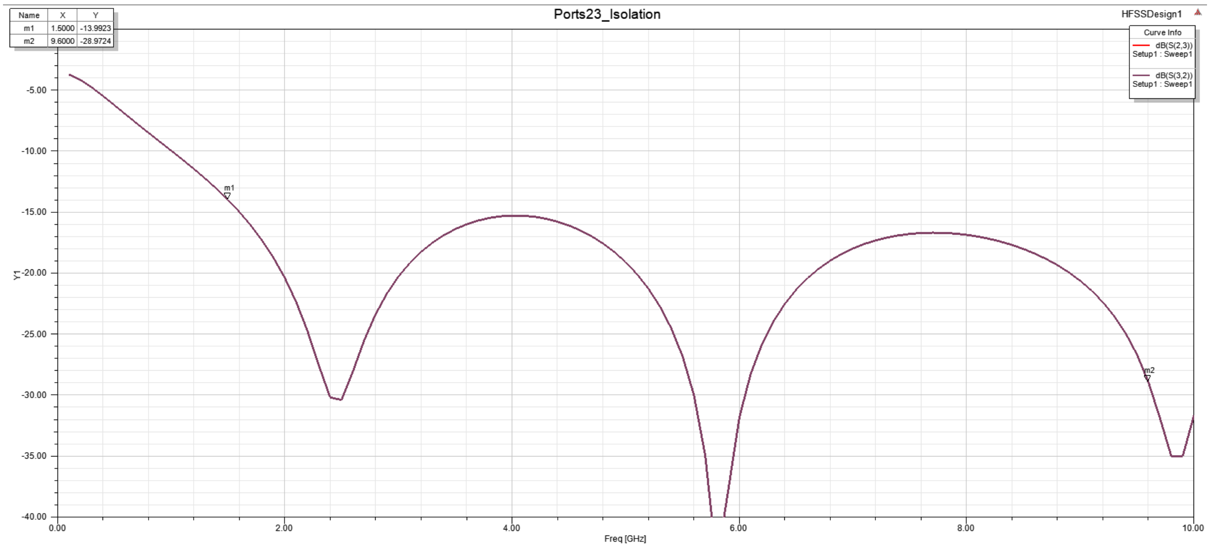

Fig. 8: Simulated results for isolation in the power divider.

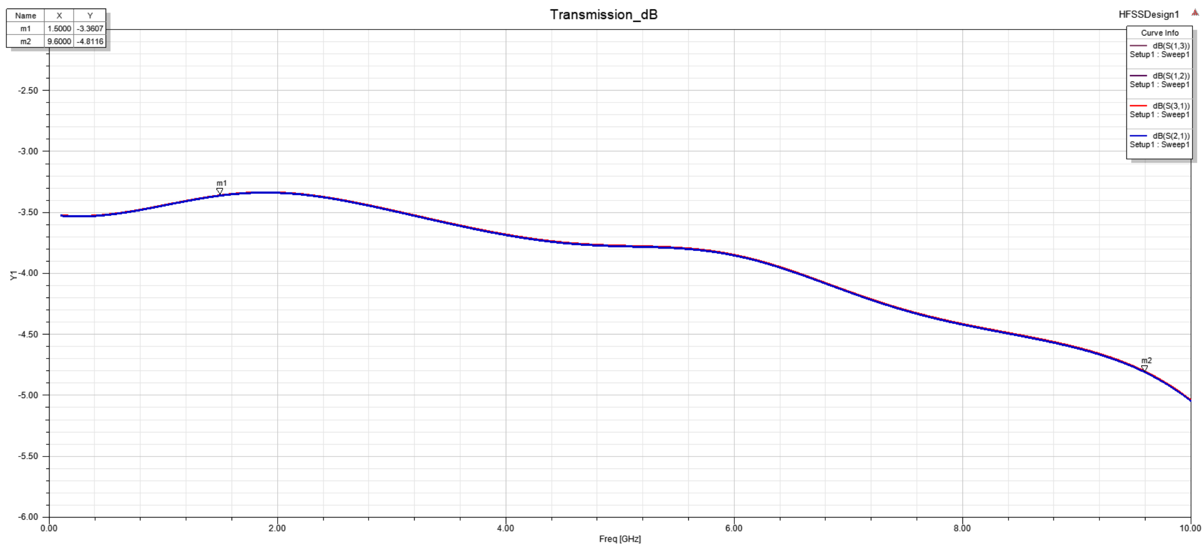

Fig. 9: Simulated results for insertion loss for the case of copper conductor and dispersive dielectric in the power divider.

4.1.3 Antenna Assembly

The antenna element was constructed for radiation pattern testing.

4.1.4 Radiation Pattern

Measurement (in open) of electromagnetic radiation pattern of the single element to characterise its response (directivity) over the bandwidth.

The radiation pattern of the antenna was measured in an open range setup. The figures below show the measured patterns from 1.2 GHz to 10.0 GHz.

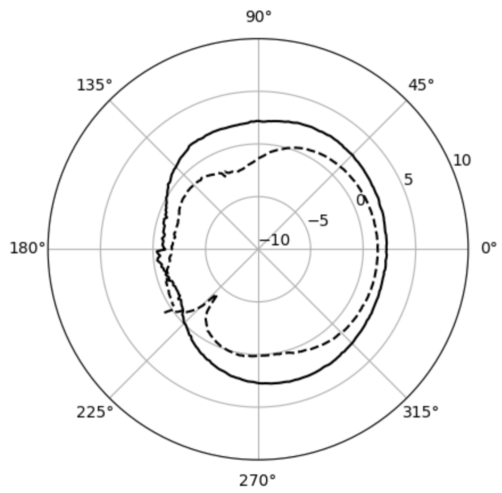

Measured at 1.2 GHz

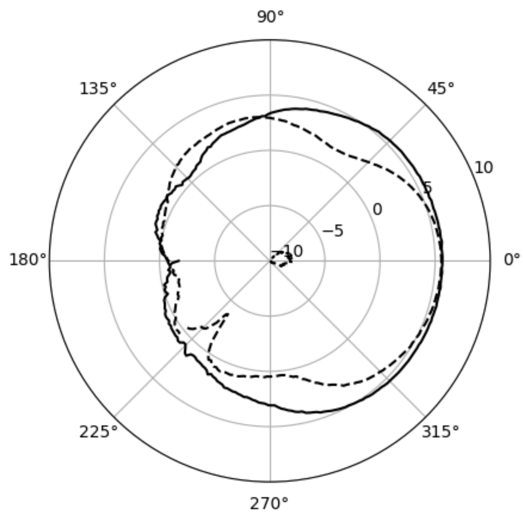

Measured at 2.0 GHz

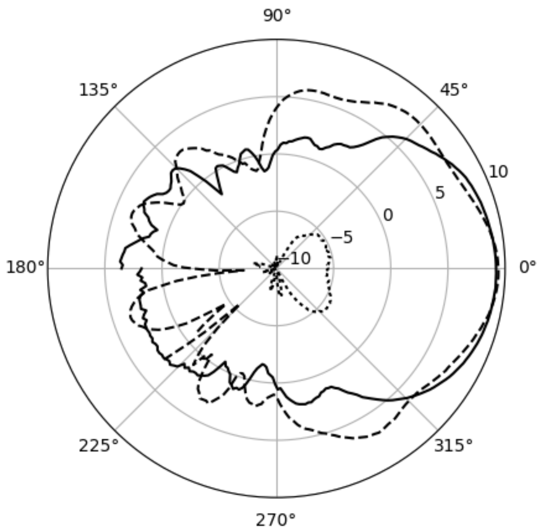

Measured at 5.0 GHz

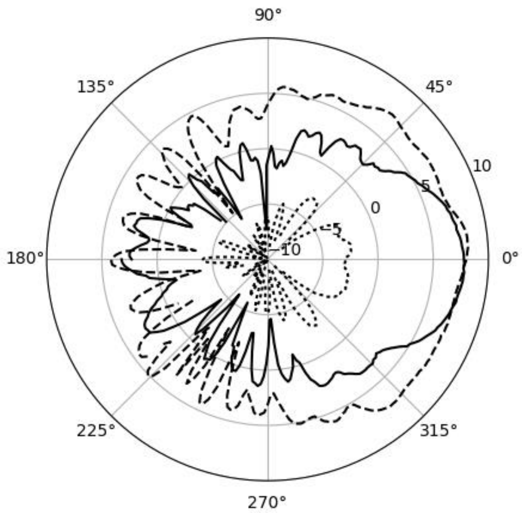

Measured at 10.0 GHz

Fig. 10: Measured radiation patterns of antenna element for 1.2, 2, 5 and 10 GHz. The solid black lines are radiation pattern in the E-plane, black dashes are the patterns in H-plane, and black dots are measured cross-polarization measurements.

4.1.5 Antenna Feed Design and Performance

Design of the array power feed, initially using uniform phase/amplitude driving signals for test purposes, combined the single power splitter design onto a single board.

The design of the antenna feed began with the objective of generating a footprint on a flat surface of a certain size at a certain distance. In the case of this design, the aim was to generate footprints of less than 20cm in diameter (in one dimension) on a flat surface, 1m from the antenna.

Using scalar diffraction equations, we computed the contributions of different configurations of antenna positions and input signals on a surface at any specified distances so that an array of Vivaldi antennas, placed at in a 42 cm row, fed with specific input signals could generate such signals at frequencies from 1 to 10 GHz.

Using the existing design of power divider, a feed structure was drawn and fabricated.

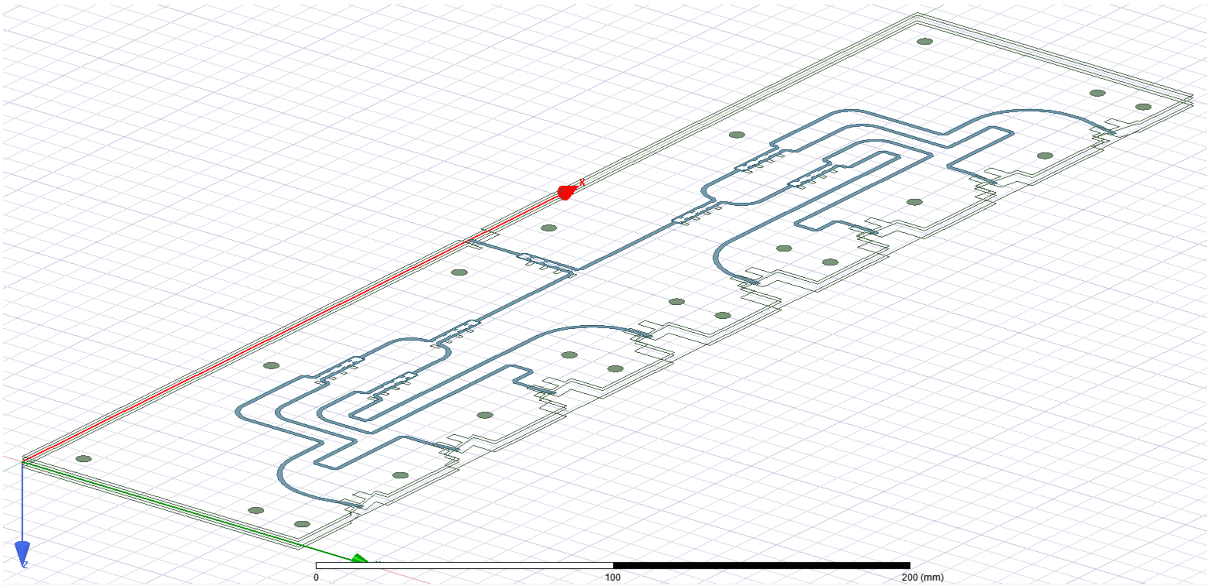

Fig. 11: Feed structure design fabricated on a PCB.

The following describes the computed radiated power that impinges onto a flat surface that is located at 1.0 m distance from the BBv2 antenna array.

Assumption:
1.0 m distance is assumed to be at 'far-field' distance. This allows the resultant E-field to be a product of array and antenna E-field contributions. Note that this is clearly not the case and gives rise to inaccuracies – there is a better estimation, but that requires significant research effort, and will be performed later.

Antenna characteristics:
- 8 elements spaced at an equal distance (6.0 cm) apart in a line array.
- Polarization direction is normal to line array.
- Elements are fed with signals at equal power, but at different time of arrivals.
- Signals that are fed to elements at the centre of the array are delayed versions of signals at the edge.
- Each element is a Vivaldi antenna with dimensions of 13 cm x 15 cm.
- Total array dimensions = 42 cm x 13 cm x 15 cm.

Simulation parameters:
- Radiated power of 1.0 m x 1.0 m planar surface at distances from 0.6 m - 1.5 m (at 0.1m intervals).
- Planar surface is simulated at a resolution of 0.01 m (1 cm) in both axes.
- Frequencies simulated are 1 GHz – 10 GHz, at 1 GHz intervals.
- Antenna radiation pattern is simulated at 2 degrees resolution.

Table 1: Footprint size at 1 m.

f (GHz)	x-size (cm)	y-size (cm)	f (GHz)	x-size (cm)	y-size (cm)
1.0	126	54	6.0	122	8
2.0	106	28	7.0	119	8
3.0	75	18	8.0	126	6
4.0	69	14	9.0	98	6
5.0	61	10	10.0	181	4

Table 2: Footprint size at 5GHz, and from 0.6m to1.5m distance.

Distance(m)	0.6	0.7	0.8	0.9	1.0	1.1	1.2	1.3	1.4	1.5
x-size(cm)	37	42	47	54	61	66	71	79	85	91
y-size(cm)	8	8	8	10	10	12	12	14	14	16

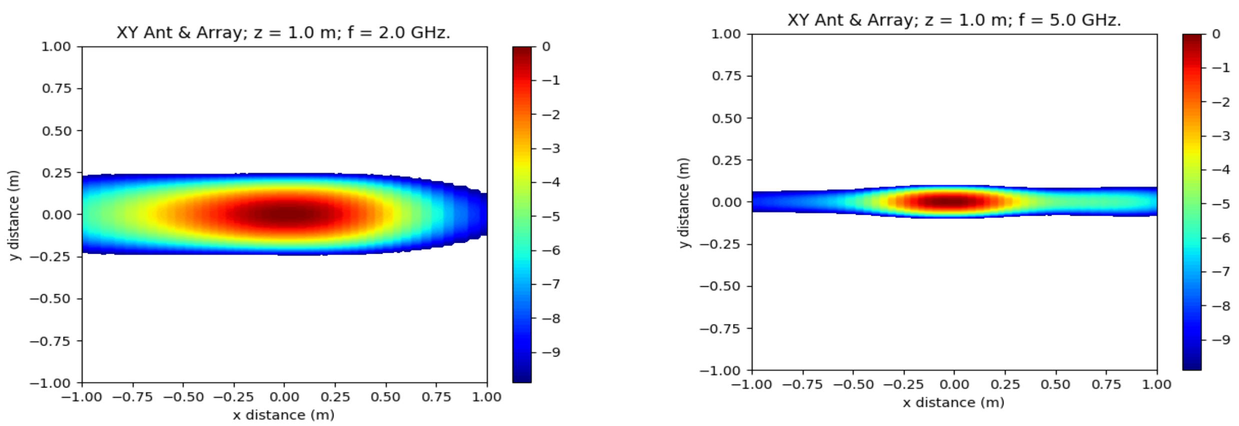

Fig. 12: Antenna array footprint size at 1m and for 2 and 5 GHz.

4.2 Milestone 3 – Live Carcase

4.2.1 Phantom Design & Construction

The design and construction of artificial sheep fat and muscle layer representing their dielectric properties – for use in laboratory experiments. Four phantoms sheep segments using this material, constructed in moisture isolating masks, represent the fat depth values of 0, 9, 23 and 38 mm. A further 2 muscle layers were completed ready for applying artificial fat, prior to the project stopping.

Table 3: From Gabriel, S. et al., 'The dielectric properties of biological tissues: II. Measurements in the frequency range 10 Hz to 20 GHz', Phys. Med. Biol. 41, 2251 (1996).

Dielectric values at 10 GHz and 37 °C		
Tissue	ε_r	σ (S m^{-1})
Heart muscle (bovine)	40	13
Muscle (across, bovine)	41	13
Muscle (along, bovine)	46	11
Adipose tissue (ovine)	6.6	1.6

We then designed a container whose diameter approximated that of the antenna beam into which we poured a “muscle” bases and followed by a “fat” layer with a specified depth of 0, 9, 23 and 38 mm versions, Fig. 13, 14.

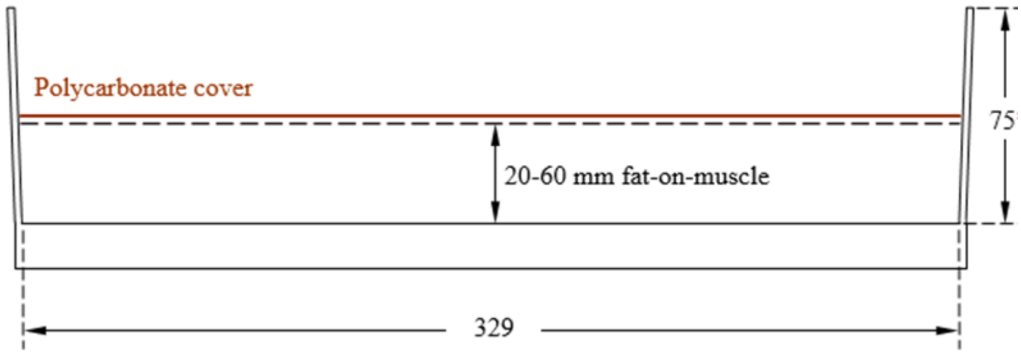

Fig. 13: PVC former and muscle/fat fill for phantoms.

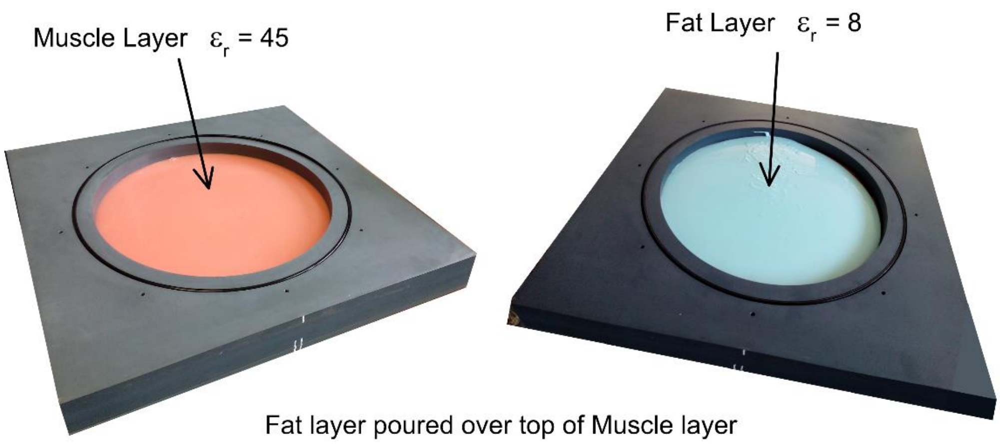

Fig. 14: Phantom target #3 – 1.9 cm fat layer poured over the top of a muscle layer.

4.2.2 Phantom Calibration

Dielectric calibration of the above constructed layers using a dielectric probe. This step validated the complex permittivity (dielectric constant and loss factor) over 6 to 12 GHz.

We then determined that the most practical method for making the phantom tissue was from Lazebnik, M. et al., Phys. Med. Biol. 50, 4245 (2005) who stated: “We propose and characterize oil-in-gelatin dispersions that approximate the dispersive dielectric properties of a variety of human soft tissues over the microwave frequency range from 500 MHz to 20 GHz. Different tissues are mimicked by selection of an appropriate concentration of oil…” Following Lazebnik’s recipes we prepared samples, poured into the PVC formers, and obtained the following results.

Table 1: Measured characteristics of muscle phantom.

Comparison of 10 GHz values		
Parameter	Measured	Targets
ε_r'	37.0	41
σ (S/m)	12.3	13

Table 5: Measured characteristics of fat phantom.

Comparison of 10 GHz values		
Parameter	Measured	Targets
ε_r'	8.7	6.6
σ (S/m)	2.5	1.6

5 Discussion

N/A due to the project being terminated by Meat & Livestock Australia due to research priorities.

6 Conclusions/recommendations

N/A due to the project being terminated by Meat & Livestock Australia due to research priorities.

7 Key messages

N/A due to the project being terminated by Meat & Livestock Australia due to research priorities.

8 Bibliography

N/A due to the project being terminated by Meat & Livestock Australia due to research priorities.

9 Appendix

N/A due to the project being terminated by Meat & Livestock Australia due to research priorities.